T_{20} problem and spin observables in pion-deuteron scattering

T. Mizutani
Virginia Polytechnic Institute and State University, Blacksburg, Virginia 24061

C. Fayard and G. H. Lamot
Institut de Physique Nucléaire and Institut National de Physique Nucléaire et de Physique des Particules, Université Claude Bernard, Lyon-1, F-69622 Villeurbanne CEDEX, France

B. Saghai
Service de Physique Nucléaire-Haute Energie, Centre d'Etudes Nucléaires de Saclay, F-91191 Gif-sur-Yvette CEDEX, France

(Received 8 June 1989)

There has been a long-standing problem in the coupled πNN-NN theory concerning its apparent failure in reproducing the tensor polarization T_{20} in the elastic πd scattering at medium energies. A mechanism recently proposed by Jennings to solve this problem is examined. It is then found that it comes from the positive-energy pole in one of the nucleon propagators in the exchange impulse diagram within the covariant picture which is usually overlooked when devising the spectator on-mass-shell approximation, and that it does not lead to the claimed near cancellation of the Pauli exchange contribution, but is important to be included. The inclusion of this contribution is shown to considerably improve in reproducing the pion-deuteron spin observables including T_{20}, particularly above the delta resonance energy.

I. INTRODUCTION

The purpose of this paper is to study various spin observables in the elastic pion-deuteron scattering predicted by the coupled πNN-NN model in comparison with recent data. Of particular interest is the tensor analyzing power T_{20} (or its laboratory frame counterpart $t_{20}^{\rm lab}$) which has been quite controversial up to now regarding different model predictions as well as their confrontation with recent data.

Several years ago the coupled πNN-NN equations (hereafter referred to as PNE) were developed in order to describe the following processes in a unified manner:[1-3]

$$\left.\begin{matrix} NN \\ \pi d \end{matrix}\right\} \rightarrow \left\{\begin{matrix} NN \\ \pi d \\ \pi NN \end{matrix}\right. .$$

This required an extension of the pure three-body (or two-body) scattering equation to be coupled to the two-body (three-body) states consistently, giving a due respect to unitarity, etc. The coupling between the two- and three-body channels is accomplished by an introduction of the pion emission and/or absorption (or πNN) vertex which is closely related to the $\pi N\, P_{11}$ partial wave. This point will be discussed extensively below as it is the pivot which the whole issue of problem and solution discussed in the present paper turns around.

During the past few years there has been a considerable accumulation in the high quality experimental data in the two-body processes:

$$\left.\begin{matrix} NN \\ \pi d \end{matrix}\right\} \rightarrow \left\{\begin{matrix} NN \\ \pi d \end{matrix}\right.$$

while those with three-body final states

$$\left.\begin{matrix} NN \\ \pi d \end{matrix}\right\} \rightarrow \pi NN$$

have been increasing. This situation has made it possible to actually test the PNE model predictions. We can safely conclude that up to now the model gives, at least, a good qualitative agreement with the data in a variety of channels, see Garcilazo and Mizutani for a brief review.[4] This alone is a nontrivial attainment.

A characteristic feature of the PNE result that we have found empirically is that the πd elastic channel, which is the interest of our present paper, appears to a very good extent to be decoupled from the rest, except at very low energies. Since the deuteron is quite a loosely bound system allowing the near on-shell single scattering (impulse) process to be the major contribution (which is then dominated by the Δ resonance in the energy region of interest), this consequence seems quite reasonable and the coupling to the NN channel should stand as a small perturbation (this does not mean that the global coupling $NN \leftrightarrow \pi d$, is weak; for example there is a strong influence from the πd channel on the NN inelasticity up to $T_N^{\rm lab} \simeq 600$ MeV, see Ref. 5). Indeed, when one compared the result of the PNE model with that of the pure three-body calculation, the difference was rather small in major πd observables. They even share the failure of not reproducing such data as large angle differential cross sections and vector polarization it_{11} above the Δ resonance. However, at least in one observable, the tensor polarization T_{20}, the PNE and the three-body model differed considerably in the backward hemisphere ($\theta_{\rm c.m.} > 90°$). Clearly this difference must come from how the coupling to the NN channel is incorporated. In fact the standard three-body treatment of the πd scattering has practically

no NN coupling as will be clear in the discussion below. On the experimental side the laboratory quantity t_{20}^{lab} was one of the first πd spin observables measured[6] (later measurement of the same quantity can be found in Ref. 7) which then was compared with the models. Surprisingly enough, the less sophisticated pure three-body model[8] followed the data rather closely while the PNE result[9,10] was off at backward angles, although it should be kept in mind that the data points were yet rather scarce. So there were some repeated arguments that the PNE must be wrong and that rather the standard three-body approach should be employed for the correct description of the πd elastic process.[8] Note that this three-body model is applicable only to the πd elastic and break-up processes, but not to those which start or end with the NN state. After all this is why the PNE was called for, as mentioned above. So the situation was quite bothersome. More recently, thanks to the sufficiently tensor-polarized deuteron target, the direct measurement of T_{20}, together with other πd tensor polarizations, become feasible.[11,12] This is a drastic improvement over the measurement of the recoil deuteron polarization t_{20}^{lab} which always comes out as a linear combination of T_{20}, T_{21}, and T_{22}. Here again the global features of the data (T_{20}, τ_{21}, and τ_{22}) were qualitatively explained by three-body models, but not by PNE (note that above the Δ resonance the three-body result also deviates from those new data). Naturally, the question arose as to why the "correct" PNE model appeared to have failed in this quantity. Recently there was an attempt to solve this problem by Jennings[13,14] which appeared to be successful.

In the following sections we first give a pedagogical analysis of the problem in some detail. To some readers in the field this might sound repetitive. But we would like the present work to be self-contained to minimize the shuttling back and forth among several different publications. Then we critically examine the mechanism proposed by Jennings. We found that irrespective of whether his claim is totally correct or not this mechanism must be incorporated in the PNE calculation of the πd spin observables. Some results including the correction from this mechanism are presented, and the conclusion is drawn at the end.

II. THE T_{20} PROBLEM

As a first step in understanding the T_{20} problem let us look into the πd helicity amplitudes. Following Grein and Locher[15] we write four independent amplitudes as $A=H_{++}$, $B=H_{+0}$, $C=H_{+-}$, and $D=H_{00}$, where subscripts are the deuteron helicity in the initial and final states. Those amplitudes are functions of energy and scattering angle. In terms of them all the πd observables are proportional to the sum of their bilinear produces, as shown in Appendix A. Their characteristic features, valid even in the simplest impulse approximation, are the following (see Fig. 1).

(a) The dominant amplitudes are the helicity nonflip pieces A and D, which determine the global feature of the scattering. Both are quite large in the forward angles and decrease fast for larger angles.

(b) The helicity flip amplitudes B and C vanish at the very forward angle and remain small at all angles as compared with A and D.

(c) Only C and D are nonvanishing at $\theta_{\text{c.m.}}=180°$. In fact their magnitude increases slowly towards this very backward angle.

It is then clear that among major πd spin observables T_{20} is the only one which is not constrained to vanish at $\theta_{\text{c.m.}}=180°$, so could even be large in that vicinity (here we do not consider some of those experimental quantities like τ_{22} etc. which linearly contain T_{20}). In particular, at very large angles

$$T_{20}\simeq\sqrt{2}(|C|^2-|D|^2)/(2|C|^2+|D|^2)\ .$$

So even though (i) this observable contains no interference of two distinct helicity amplitudes and (ii) the magnitude of C and D is small, the two models (standard three-body and PNE) could give quite different T_{20} predictions provided that the difference in the model prediction $\Delta|C|=|C_{\text{PNE}}|-|C_{\text{3-body}}|$ (or the similar quantity for D) is of the same order as $|C|$ (or $|D|$) itself (from either or the models) at this angular range. Note that at smaller angles, the difference of this order of magnitude may not stand out as the dominant amplitudes are far larger. In fact this appears exactly what one has found in the model predictions: while $|C|$ is less than $|D|$ in the three-body result, PNE makes $|C|$ equal to or even greater than $|D|$ at very large angles. This is manifest in Fig. 1. As will be discussed later, we have observed that *the three-body result with and without P_{11} is almost equivalent.* We therefore show the result without P_{11} in that figure. Thus within PNE T_{20} becomes even positive in some choice of two-body input at $\theta_{\text{c.m.}}=180°$, while it stays large and negative in three-body models. It is important to mention, in passing, that this tendency can already be observed in the lowest order (impulse) approximation. What the recent T_{20} data[12] tell us is that for certain pion kinetic energies $T_{20}(180°)$ approaches very close to the unitary limit $-\sqrt{2}$. This means that at large angles $|C|$ is certainly less than $|D|$, thus apparently the three-body result is favored. In the following we shall look more closely into the origin of the difference in the T_{20} prediction by those models.

As may be clear from how the original PNE was constructed in extending the three-body equation,[1] the difference consists in how the pion emission and absorption is implemented through the πN P_{11} partial wave. Although the following argument may be familiar,[16] we would like to repeat it for clarity. Briefly, to be consistent with the πN partial wave analysis, the input P_{11} amplitude to the three-body equation (or PNE) must consist of two parts. The (s-channel) nucleon pole term is made up of two πNN vertices connected by the nucleon propagator [Figs. 2(a)]. This gives a repulsive contribution which is compensated by the remaining piece called the nonpole part [Fig. 2(b)], to make the whole P_{11} amplitude weakly repulsive up to $T_\pi^{\text{lab}}\simeq 200$ MeV. From unitarity and analyticity it was proven that the nonpole part is unitary by itself while the vertices and propagators in the pole term must have dressing by the virtual pions

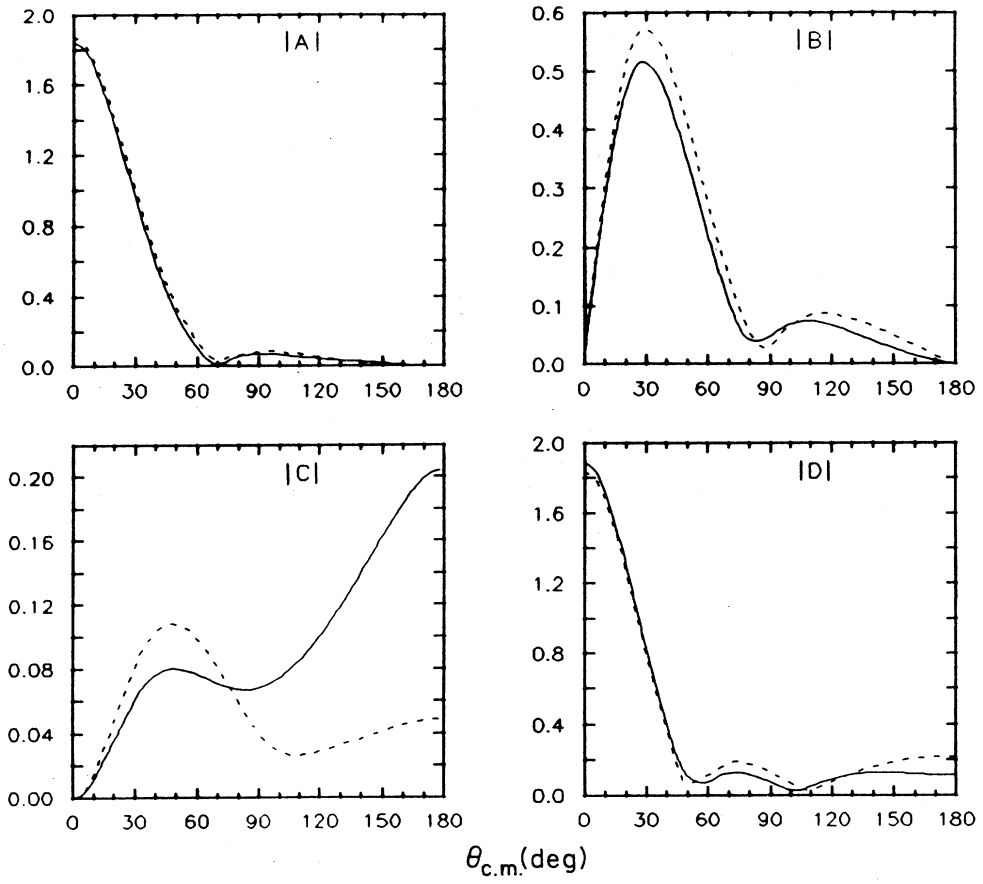

FIG. 1. Moduli of the πd helicity amplitudes $|A|$, $|B|$, $|C|$, and $|D|$ (in fm) calculated at $T_\pi^{lab}=256$ MeV. Curves are standard πNN-NN theory (PNE) of Ref. 10 (full line), and pure three-body result without the P_{11} contribution (dashed line).

such that the sum of those two terms be unitary.[16] Formally this decomposition is *unique* contrary to the statement by Jennings.[13] However, the magnitude of the pole and nonpole terms cannot be determined unambiguously by exploiting only the elastic πN information (the elastic πN data only constrain the sum of those two terms which is, as already stated above, weakly repulsive). In this sense the actual decomposition of this partial wave at present appears not unique. Yet, close to the elastic threshold, the nucleon pole position and the value of the πNN coupling constant tightly constrain the pole term so the ambiguity may be considered under control (for both the pole and nonpole terms). Also it is quite possible that the magnitude of the pole term (and thus that of the nonpole part as well) may be large as inferred from the tree diagram in any reasonable (effective) chiral Lagrangian model of mesons and baryons.

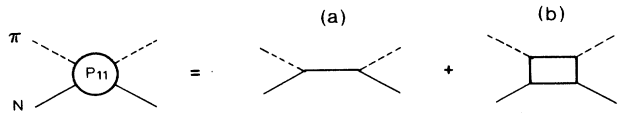

FIG. 2. Decomposition of the πN P_{11} amplitude into pole (a) and nonpole (b) parts.

In the πNN system this P_{11} amplitude serves as one of the two-body input elements driving the multiple scattering (or successive binary collisions) among the pion and two nucleons. So, at first sight, it may be natural to think that only the total (viz. the pole and nonpole terms in combination) P_{11} amplitude should always appear in the multiple scattering series. The consequence of this is of course the standard three-body treatment where no pole and nonpole separation is needed. However, in the presence of a spectator nucleon, the propagating nucleon found in the P_{11} pole term must respect the Pauli principle. Therefore the P_{11} amplitude in the πNN system must be modified due to the proper antisymmetrization of the two nucleons. This modification is correctly implemented in PNE, which then allows the simultaneous description of reactions like $NN \leftrightarrow \pi d$, $NN \rightarrow NN$, etc. To understand this point more clearly we consider the impulse πd term through the πN P_{11} wave. This is appropriate as our present discussion is confined within the πd elastic process. The contribution is depicted in Fig. 3. In the three-body model only diagrams (*a*) (pole contribution) and (*b*) (nonpole contribution) enter which, in combination, give very small contribution as anticipated from the small P_{11} amplitude. In fact, together with the dominant P_{33} wave input, the P_{11} contribution in this

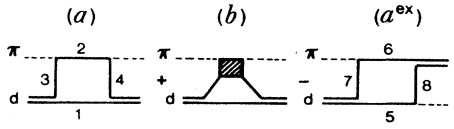

FIG. 3. The impulse contribution to the πd scattering through the P_{11} wave. Diagram (a): pole contribution; diagram (b): nonpole contribution; diagram (a^{ex}): exchange term to (a). The same notations are used in the text for the amplitudes corresponding to these diagrams. In the case of relativistic off-mass-shell description, the nucleon propagators are numbered from 1 to 8.

form is almost negligible. *For this reason the results of three-body calculations with and without P_{11} are almost identical.* Now in the PNE description there is an additional term (a^{ex}) [see Fig. 3], which is the Pauli exchange counterpart to diagram (a) with a negative sign. Qualitatively, when ignoring the spin complication, amplitude (a) is forward dominated in its angular dependence and thus its Pauli exchange counterpart (a^{ex}) is backward dominated as a consequence. By an explicit calculation of (a) and (a^{ex}) we have found that this tendency: $|(a^{ex})|$ equals the mirror image of $|(a)|$ with respect to $\theta_{c.m.}=90°$, holds approximately upon introducing the spin degrees of freedom. In our present context this may quite well cause the difference in $|C|$ and $|D|$ by the two models, as discussed above.

Upon partial wave decomposition one finds for a given J^π combination of total angular momentum and parity

$$(a)_{l'l}=(a)_{l'l}[\text{per}]+(a)_{l'l}[fb]\ , \tag{1}$$

and

$$(a^{ex})_{l'l}=-(a)_{l'l}[\text{per}]+(a)_{l'l}[fb]\ . \tag{2}$$

In the above expressions l and l' are the initial and final orbital angular momenta, and [per] and $[fb]$ signify the parts which go through Pauli-*permitted* and -*forbidden NN* states, respectively. For certain πd J^π states the Pauli-permitted part of (a) vanishes, while for some other J^π the corresponding Pauli-forbidden part becomes zero. Then the total impulse contribution through the P_{11} in partial wave J^π reads

$$2(a)_{l'l}[\text{per}]+(b)_{l'l}\ , \tag{3}$$

or

$$(b)_{l'l}\ . \tag{4}$$

This point may be more easily understood by looking into Table I where the first few πd partial waves and the *NN* partial waves that couple to them are listed. Also indicated in the table is whether those *NN* waves are either Pauli allowed or forbidden. Then from this table it is clear within PNE that in the impulse πd scattering through the πN P_{11} wave every natural parity state and even-J unnatural parity states (except for 0^-) get the contribution as in Eq. (3), whereas the odd-J unnatural parity states receive the contribution as in Eq. (4) where no coupling to the *NN* channel is effective due to Pauli blocking. To see this, we have explicitly calculated the partial wave contributions from diagrams (a) and (a^{ex}) as found in Table II (first through fourth columns). In either case the contribution could be quite different from the three-body result,

$$(a)_{l'l}[\text{per}]+(a)_{l'l}[fb]+(b)_{l'l} \tag{5}$$

which should be quite small.

The next step is to compare the two sets of πd partial waves produced by three-body and PNE models once incorporating other πN partial wave contributions and to iterate the multiple scattering series to all orders. A typical result valid in the Δ resonance region is shown in Table III. Since the major partial waves $f^J_{J-1,J-1}$ $(J=2^+,3^-,1^-)$ are so much dominated by the $(N\Delta)l=0,1$ states, they do not show much sensitivity to the different treatment of the P_{11} wave [note that the corresponding $N-\pi N(P_{11})$ states for these πd partial waves are in relative $l=2,3,1$ states, respectively]. As for $f^J_{J+1,J+1}$ and nondiagonal $f^J_{J\pm1,J\mp1}$, more sensitivity to the P_{11} treatment is observed due to the reduction in the modulus of the amplitude caused by the higher πd orbital angular momentum barrier. The most striking difference is clearly observed in the 0^+ amplitude. Here the $N\Delta$ is only in $l=2$ state while the $N-\pi N(P_{11})$ is in $l=0$. However, the influence of this partial wave on various observables is not strong as it only appears in helicity amplitude D with a geometrical factor $J+1$ (see Appendix A for the relations between the helicity amplitudes and the

TABLE I. πd partial waves state and the corresponding *NN* waves which couple to them.

J^π	πd state		*NN* state			Pauli
	S	L	S	L	State	
0^+	1	1	0	0	$^1S_0$	Allowed
1^-	1	0,2	1	1	$^3P_1$	Allowed
			0	1	$^1P_1$	Forbidden
2^+	1	1,3	1	2	$^3D_2$	Forbidden
			0	2	$^1D_2$	Allowed
3^-	1	2,4	1	3	$^3F_3$	Allowed
			0	3	$^1F_3$	Forbidden
0^-	no	no	1	1	$^3P_0$	
1^+	1	1	1	0,2	$^3S_1$-$^3D_1$	Forbidden
2^-	1	2	1	1,3	$^3P_2$-$^3F_2$	Allowed
3^+	1	3	1	2,4	$^3D_3$-$^3G_3$	Forbidden

TABLE II. πd partial wave t matrix $t^J_{ll'}=t^J_{l'l}$ from diagrams (a), (a^{ex}), and (c) at $T_\pi^{lab}=142$ MeV. Deuteron used has only S-wave component. In the four columns marked * the nucleon self-energy by the virtual emission of a single pion is included for the intermediate states, and a monopole πNN vertex with a cutoff mass of 800 MeV/c is used in calculating this self-energy. The normalization of the partial wave amplitudes is the same as in Ref. 10. Notice the degree of cancellation here.

J	l	l'	*Re(a)	*Im(a)	*Re$(-a^{ex})$	*Im$(-a^{ex})$	Re$(-a^{ex})$	Im$(-a^{ex})$	$-c$
0	1	1	190.80	−49.52	190.80	−49.52	372.90	−4.24	−326.20
1	0	0	51.99	−11.59	17.33	−3.86	32.73	−0.05	−30.38
1	2	0	0.00	0.00	49.02	−10.93	92.59	−0.13	−85.91
1	1	1	131.40	−33.99	−131.40	33.99	−256.60	2.84	225.30
1	2	2	51.99	−11.59	−17.33	3.86	−32.73	0.05	30.38
2	1	1	12.58	−2.93	−2.52	0.59	−4.80	0.01	4.71
2	3	1	0.00	0.00	−12.33	2.87	−23.52	0.04	23.09
2	2	2	32.57	−7.28	32.57	−7.28	61.56	−0.09	−57.32
2	3	3	12.58	−2.93	2.52	−5.86	4.80	−0.01	−4.71
3	2	2	3.43	−0.82	0.49	−0.12	0.94	0.00	−0.94
3	4	2	0.00	0.00	3.40	−0.81	6.54	0.00	−6.53
3	3	3	7.62	−1.78	−7.62	1.78	−14.6	0.02	14.30
3	4	4	3.43	−0.82	−0.49	0.12	−0.94	0.00	0.94
4	3	3	1.01	−0.24	−0.11	0.03	−0.22	0.00	0.22
4	5	3	0.00	0.00	−1.00	0.24	−1.93	0.00	1.95
4	4	4	2.04	−0.49	2.04	−0.49	3.94	0.00	−3.94
4	5	5	1.01	−0.24	0.11	−0.03	0.22	0.00	−0.22

partial wave amplitudes $f^J_{l'l}$). There is also a very clear manifestation of the different P_{11} treatment in 1^+ wave since the contribution from the P_{11} pole part, which is in $(NN)l=0$, is completely Pauli blocked in PNE. This leaves a strong attractive piece due to the nonpole part. As stated earlier this blocking occurs in all odd-J unnatural parity waves, but the difference between PNE and the three-body becomes smaller rapidly with increasing J. According to the formulas in Appendix A, these unnatural parity amplitudes contribute only to helicity amplitudes A and C, but at large angles only C is relevant. So one might expect that this difference should be reflected in C and that one could find the key to the solution in the T_{20} problem. With this in mind we have replaced all unnatural parity partial wave amplitudes in the PNE model by those from the three-body model. The result is a noticeable decrease in $|C|$ at backward angles. This has been achieved to a good extent by the 1^+ amplitude but

TABLE III. πd partial wave amplitudes at $T_\pi^{lab}=142$ MeV from the PNE model of Ref. 10 and the pure three-body result without the $\pi N P_{11}$ input.

J	l	l'	P_{11}		No P_{11}	
0	1	1	330.35	−224.52	−85.71	−182.28
1	0	0	6.64	−552.16	−36.36	−544.96
1	0	2	−46.45	−64.39	−82.40	−90.39
1	1	1	−253.23	−756.60	−274.16	−501.56
1	2	0	−46.45	−64.39	−82.40	−90.39
1	2	2	−85.87	−151.86	−18.22	−77.52
2	1	1	−537.37	−1408.10	−750.77	−1450.00
2	1	3	8.97	18.64	21.61	43.84
2	2	2	−144.49	−254.62	−231.58	−276.72
2	3	1	8.97	18.64	21.61	43.84
2	3	3	−9.26	−37.82	−9.82	−27.28
3	2	2	−328.24	−381.96	−344.00	−379.63
3	2	4	17.67	16.83	10.56	13.95
3	3	3	−87.71	−93.12	−60.96	−76.47
3	4	2	17.67	16.83	10.56	13.95
3	4	4	−6.29	−14.14	−3.28	−9.42
4	3	3	−86.03	−98.35	−86.33	−97.36
4	3	5	1.37	2.53	2.79	3.21
4	4	4	−12.12	−23.38	−15.77	−22.80
4	5	3	1.37	2.53	2.79	3.21
4	5	5	−0.98	−4.42	−0.96	−3.29

that alone is by no means sufficient: a certain coherence due to several of those waves seems to be needed. As for T_{20} this change in C is still insufficient to bring it down to sufficiently negative value, within the PNE. To find a satisfactory T_{20} at large angles it is necessary to have large $|D|$ relative to $|C|$. For the reason stated above this cannot be done by the change in the unnatural parity partial waves alone. By numerical experiment we have found that all the 1^-, 2^+, 3^- large and small partial waves in the PNE model also must be replaced by their three-body counterpart.

The conclusion concerning this matter is that in one way or another the issue appears to be related to the treatment of the Pauli principle. The real trouble is that the model with "an apparently proper consideration" of the Pauli principle is inferior to the one without it. So there appeared some rumor that some people even questioned the effectiveness of the Pauli principle for off-shell nucleons. But what is then the real origin of this apparent suppression of the Pauli principle?

III. STUDY IN THE JENNINGS MECHANISM

Recently in an attempt to resolve the above-mentioned problem Jennings proposed an interesting idea[13] which apparently did not require any exotic ingredient like the violation of Pauli principle by off-shell nucleons as referred to above. His arguments is that in the time-ordered formalism, the diagram (c) shown in Fig. 4 largely cancels the diagram (a^{ex}) of Fig. 3, thus effectively lifting up the Pauli principle (Jennings introduced this diagram as the Pauli exchange counterpart of the diagram shown in Fig. 5, which is predominantly in $\pi N\, P_{33}$ wave in the presence of the nucleon spectator).

Later, within a simplified model, Jennings and Rinat[14] demonstrated that the addition of this extra diagram to the πd amplitude obtained from the PNE did restore the agreement with the experimental T_{20} while giving very slight change to the remaining observables. They expected that the near cancellation could as well take place in higher order but that, hopefully, these higher order contributions might be small. This remains a mere conjecture. Clearly, this extra contribution (c) involves an explicit four ($\pi\pi NN$) particle state so it does not seem to be generated either in the conventional three-body (πNN) or PNE model. Thus these authors concluded that the T_{20} trouble is just a manifestation of the shortcoming of the coupled πNN-NN (PNE) theory.

In view of its potential importance in the πNN problem in general we have reexamined the claims of Jennings and Rinat. The conclusion we have reached is presented below.

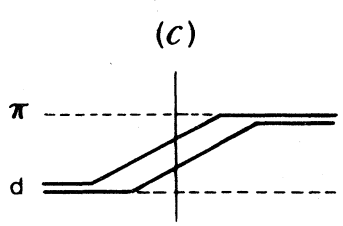

FIG. 4. The diagram (c) suggested by Jennings. The vertical line is to indicate that the intermediate state has four particles.

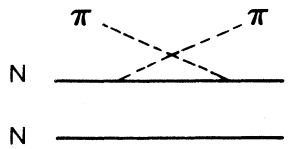

FIG. 5. The u-channel nucleon pole term in the presence of a spectator nucleon. The Jennings term originally proposed (Fig. 4) is just the Pauli exchange partner of this term.

(i) Cancellation. We shall first examine the claim of the near cancellation between diagrams (a^{ex}) and (c). Within the time-ordered theory as discussed by Jennings it is clear that diagram (c) gives a purely real contribution, whereas (a^{ex}) is complex as the intermediate NN state is above its elastic threshold whenever the incoming πd state is physical. So already at this stage one knows that their exact cancellation is impossible. Jennings appears to have disregarded the imaginary part. So the question is twofold: (1) if the imaginary part of (a^{ex}) is quite small, and (2) if the real part of (a^{ex}) and (c) nearly cancel. This has been tested and we found the same conclusion as Jennings as long as no consideration of the nucleon self-energy is given (See Table II, fifth and seventh columns). However, in the Δ resonance region the self-energy effect becomes important (this is related to the unitarity of the πN-P_{11} amplitude). And with the inclusion of this effect the imaginary part of (a^{ex}) becomes of the same order of magnitude as its real part, and the near cancellation of Re[(a^{ex})] and (c) is now gone (third and seventh columns in Table II). Note that when calculating the nucleon self-energy we only considered the virtual emission of a pion that is the only relevant process at the energies of our present interest. Also we employed a monopole cutoff of 800 MeV/c at the πNN vertex which gives a somewhat conservative but reasonable estimate of the self-energy effect. Our conclusion is that although the near cancellation cannot be expected, we should still include diagram (c) as its magnitude is of the same order as that of (a^{ex}) and it tends to compensate Re[(a^{ex})], thus partially reducing the Pauli effect due to (a^{ex}).

(ii) Need to go beyond πNN state? If diagram (c) really is the major solution to the T_{20} problem for PNE, that should be an indication that PNE is insufficient in that it does not accommodate explicit four-body $\pi\pi NN$ intermediate states, as remarked by Jennings and Rinat.[14] Then a legitimate question to ask may be if there is any model which goes beyond PNE by incorporating the $\pi\pi NN$ states. There is, in fact, a candidate for that: a set of coupled equations for the πNN-NN system developed by Stelbovics and Stingl.[17] The equations were derived in the standard time-ordered formalism by exploiting a simple model field theory containing only the two nucleons and pions. The only allowed interaction was the πNN vertex for the pion emission and absorption, and for the system of nucleons the maximum number of pions was restricted to two by the projection method. A peculiar feature of this model is that it contains disconnected interactions X and Y as driving terms, as shown in Fig. 6. Clearly, diagram Y generates (c) as the lowest order contribution to the elastic πd process. Furthermore, the

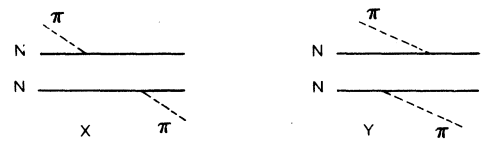

FIG. 6. Disconnected driving terms in the πNN equations of Ref. 17.

equations do formally reduce to PNE on disregarding interaction Y, as has been demonstrated by Afnan and Stelbovics.[18] So at first glance this appears to be the right model to watch. However, there are several serious drawbacks which make this model unattractive for further pursuit. First, in spite of the very simplifying assumption the equations are quite complicated and it appears to be very difficult to make it more realistic by, for example, implementing the NN heavy meson exchange interactions. Second, even if this is technically solved there still are problems which the iterations of Y together with other interactions generate: (i) the πNN vertices and nucleon self-energy terms cannot be consistently renormalized in the presence of the spectator nucleon, see Fig. 7 for example, and (ii) some noniterative NN interactions by pion exchanges are already incorporated effectively in terms of meson and vertex cutoff parameters in the adopted NN potential model. This will cause a double counting problem.

Yet there is one positive outcome from having looked at this model: as stated above some portions of the iterates containing interaction Y are to be attributed to the vertex dressing, nucleon self-energy, and noniterative pion exchange NN potentials which must be regarded as being already taken into account at the level of choosing the input to the equations. In fact the iterates belonging to this class of contributions are quite large. What this implies is that in the correct theory the contribution from Y higher than (c) may not be very important.

The failure of the Stingl-Stelbovics model, especially from the consistency point of view, stems from the time-ordered formulation which the model is based upon. It is clear that within a covariant formalism such a problem should not occur. Once adopting the covariant picture, the immediate consequence is that in terms of Feynman diagrams (a^{ex}) and (c) come out of a single diagram. So it is reasonable to guess that the $\pi\pi NN$ four-particle states in the context of Jennings may naturally be taken care of when the covariance is preserved in PNE, see third paper in Ref. 1 for a covariant derivation of PNE. Then the T_{20} problem may no longer come up. At this point we should be reminded that to the best of our knowledge all the *relativistic* three-body or PNE models

FIG. 7. Typical processes in the πNN equations of Ref. 17 that cannot be consistently renormalized.

to date have adopted the so-called *spectator on-shell approximation*.[8] This reduces the four-dimensional integral to that of three and eventually makes the form of the equations very close to that of the nonrelativistic time-ordered theory. Although part of the raison d'être of this approximation originated from avoiding the abnormal solution to the two-body relativistic bound state equation[19] as well as to have a correct one-body limit when one of the particles gets infinitely heavy,[20] its adaptation to scattering problems is largely dictated by practicality: a four-dimensional three-body scattering equation is impossible to handle. However, in our present context we have felt it necessary to reexamine its relevance.

Since our present interest is to study the Jennings mechanism, we shall concentrate on diagrams (a) and (a^{ex}) within the covariant picture. We now reinterpret Fig. 3 within that context. There the closed boxes represent off-shell nucleon propagators along which four-dimensional momentum integrations are to be done. External lines represent on-shell particles. We then number the nucleon propagators as 1–8 [$1\rightarrow4$ for (a) and $(5\rightarrow8$ for (a^{ex})] as in Fig. 3. To make the argument simple and transparent we simply state the result while somewhat more quantitative discussion is relegated to Appendix B. Now we perform a Cauchy integration in the energy variable, closing the contour in the lower half complex plane. For diagram (a) only propagator 1 gives the positive-energy pole contribution inside the closed contour, while the remaining contribution comes from the negative-energy poles and is thus suppressed. The spectator on-mass-shell approximation is just to take this positive-energy contribution. We remark again that this approximation parallels the time-ordered approach. With diagram (a^{ex}) the situation is different. In fact it admits two positive-energy poles. The first one is from propagator 5 and is the exchange counterpart of the (spectator on-mass-shell) contribution to (a) just mentioned above. So this part has been included in the PNE, causing the T_{20} problem. The second, on the other hand, is from propagator 8 and has never been considered before; this has simply been overlooked due to the very spectator on-mass-shell picture. We stress that there is no reason to believe that this latter contribution is of minor importance as compared with the first one. A close look at this term has revealed that it is what Jennings advocated to include in the πd amplitude: diagram (c). Its origin is therefore not outside the coupled PNE. Our suspicion regarding the inappropriate treatment of the Pauli principle in PNE has thus turned out to be right: the Pauli exchange term was incomplete. However, we must keep in mind that this does not give any preference to the standard three-body approach over the PNE method concerning the description of the elastic πd process, since the former disregards completely the Pauli principle.

IV. πd OBSERVABLES

Upon identifying the origin and potential importance of the so-far-missing contribution originally proposed by Jennings, we shall try to include it in our PNE calcula-

tion of the πd observables. Ideally, one solves the covariant PNE equations (the last paper in Ref. 1) which naturally include this kind of contributions to all orders. But this seems impossible. So one may calculate the leading order correction covariantly in a way discussed in the preceding section. What has not been taken into account in that discussion is the structure of the vertices and nucleon self-energy. For an actual calculation this certainly has to be taken into account. Reliable covariant models for the vertices, in our opinion, do not seem to be available yet. In such a circumstance we cannot be very ambitious but are obliged to stay rather modest. We thus calculate diagram (c) in a time-ordered model and add it to the πd amplitude from the PNE model. We could have added the second term in Eq. (B14) in Appendix B but have chosen not to do so in the present work in view of what has been just mentioned above. Basically, this is the strategy adopted by Jennings and Rinat.[14] Our first objective is to check if their finding can be qualitatively reproduced. The second objective is to study the effect of the additional diagram not only in T_{20} but also in other πd spin observables. Our inputs are different from those in Ref. 14. The first such difference is in the πNN vertex: a simple static vertex without cutoff factor was adopted. This should be plausible as the pion is on shell. We actually reached this conclusion after employing several vertices with different but reasonable cutoffs. There is one sophistication over the model of Jennings and Rinat: we have taken into account the D-state component of the deuteron. At first sight this state did not look important. But a close examination has revealed that without it diagram (c) gives no contribution to B helicity amplitude [equivalently this comes from the vanishing (c) contribution to πd spin amplitude $M_{\pm 1,\mp 1}$]. This has an important consequence in some of the spin observables as they are proportional to the real or imaginary part of the interference between B and combination of the other helicity amplitudes, see Appendix A.

The spin amplitude in the πd c.m. system corresponding to the analytic expression of diagram (c) reads

$$T_{MM'}(\mathbf{p},\mathbf{q})=\frac{-3}{8\pi^3\sqrt{\omega_p\omega_q}}\left[\frac{f_\pi}{\mu}\right]^2\int d\mathbf{k}\frac{\Psi_M^*(\mathbf{k}+\mathbf{q}/2)(\sigma_1\cdot\mathbf{p})(\sigma_2\cdot\mathbf{q})\Psi_{M'}(\mathbf{k}-\mathbf{p}/2)}{-\omega_p+E_p^d-E_N[\mathbf{k}+(\mathbf{p}+\mathbf{q})/2]-E_N[\mathbf{k}-(\mathbf{p}+\mathbf{q})/2]}\ . \tag{6}$$

Here the total c.m. energy is $\omega_p+E_p^d=\omega_q+E_q^d$, f_π is the πNN coupling constant, μ the pion mass, E_N is the nucleon energy in the intermediate states, and Ψ_M is the deuteron wave function with spin projection M. The factor -3 in the numerator comes from the isospin recoupling. The normalization of the t matrix is such that

$$f_{MM'}=-\pi\left[\frac{1}{E_p^d}+\frac{1}{\omega_p}\right]^{-1}T_{MM'}\ , \tag{7}$$

with $|f_{MM'}|^2$ being the differential cross section for the deuteron spin transition $M\rightarrow M'$ by the pion scattering.

The results are presented in Figs. 8–10 for $T_\pi^{\rm lab}=142$, 256, and 294 MeV, respectively, together with the recent data[11,12] on polarizations T_{20}, τ_{21}, τ_{22}, etc. Also included are the "data" for T_{21} and T_{22}. They were deduced from the T_{20}, τ_{21}, and τ_{22} data with appropriate error bars (note that τ_{21} and τ_{22} are linear combinations of T_{2i}, $i=0,1,2$). There are four different theoretical curves in the figures. They correspond to our PNE result without the (c) correction (dotted line), PNE plus the correction with an S-wave deuteron (dashed line), PNE plus the correction with $S+D$ deuteron (calculated from the Ernst-Shakin-Thaler approximation to the Paris potential[21]) (solid line), and the result of the pure three-body model without the πN P_{11} input (dash-dotted line). Also plotted in Fig. 11 are the moduli of the helicity amplitudes $|C|$ and $|D|$ at 256 and 294 MeV in comparison with the result of the recent amplitude analysis.[22]

One immediately finds that at 142 MeV the effect of the correction to PNE is not very noticeable and so the improvement is just insufficient: a disappointment. This is rather different from what Jennings and Rinat found,[14] to which we shall come back later. On the other hand, one observes a considerable improvement in various spin observables at the two higher energies, including $d\sigma/d\Omega$, it_{11}, etc. which have been so hard to improve so far. In particular, a remarkable improvement in T_{20} is noteworthy: one observes a wild difference between the pure PNE and the corrected ones.

Remembering the simplicity of our model input for (c) it is safe to conclude that the success we have witnessed above is an indication that basically our procedure for correcting the original PNE is in the right direction. Yet what remains bothersome is the result of 142 MeV that cannot really be viewed as a success. There are a couple of points to be investigated regarding this subject matter. First, we have found that as a function of the pion energy the improvement becomes better the higher the energy, above the Δ resonance. From a somewhat different viewpoint this may be restated as follows: the Δ dominance is manifest in the $J^\pi=2^+$, $l=l'=1$ partial wave which becomes less and less important above the resonance energy relative to $J^\pi=0^+,1^-,1^+$ partial waves which diagram (c) affects most. On the other hand the energy dependence of (c) is quite smooth. This gives us some hint as to which direction the model may be improved. For example, the next order process corresponding to diagram (c) (see Fig. 12) which proceeds through the formation of a Δ before (or after) may bring in a reasonable energy dependence to solve the problem below the resonance. Second, apparently Jennings and Rinat had no problem in attaining a qualitative agreement with the T_{20} data at 142 MeV. Their result at 256 MeV appears to be fine, too. So does this mean that there is a better model? It may be useful at this point to briefly review this model. The background PNE amplitudes were taken from Flinders[2] and Rehovoth.[3] The Flinders PNE

is a model which reproduces various observables in πd elastic, πd-NN, and NN-NN reasonably. Apart from a somewhat poor agreement with the data in πd elastic differential cross section at $T_\pi^{\text{lab}}=142$ MeV, a problem is that the splitting of the P_{11} pole and nonpole terms is not unitary (the πNN vertex is real). This eventually makes the absolute values of the pole and nonpole terms reduced, the consequence of which is the reduction of the T_{20} at large angles to become negative. In fact when this nonunitary decomposition was corrected, the resulting T_{20} became positive, just like what our model shows.[9] Regarding the Rehovoth amplitude, again the key point is the P_{11} model adopted. It implements a unitary decomposition of the pole and nonpole terms. But its prediction for the πd-NN cross section is about 30–40 % lower than the data. This indicates that the contribution from (a) and (a^{ex}) is reduced to end up with negative T_{20} at backward angles. When combined with the (c) correction both models thus have produced reasonable T_{20} at 142 MeV. Therefore one cannot conclude that the Jennings-Rinat model is better than the present one. Since the Flinders PNE model amplitudes were available, we adopted them in combination with our (c) contribution, see Figs. 13 and 14. Indeed, the 142-MeV T_{20} came out nicely. When compared with our result some observables like T_{22} are rather similar above the resonance energy. However, it_{11}, after correction, gets completely deteriorated while the same quantity in our result has im-

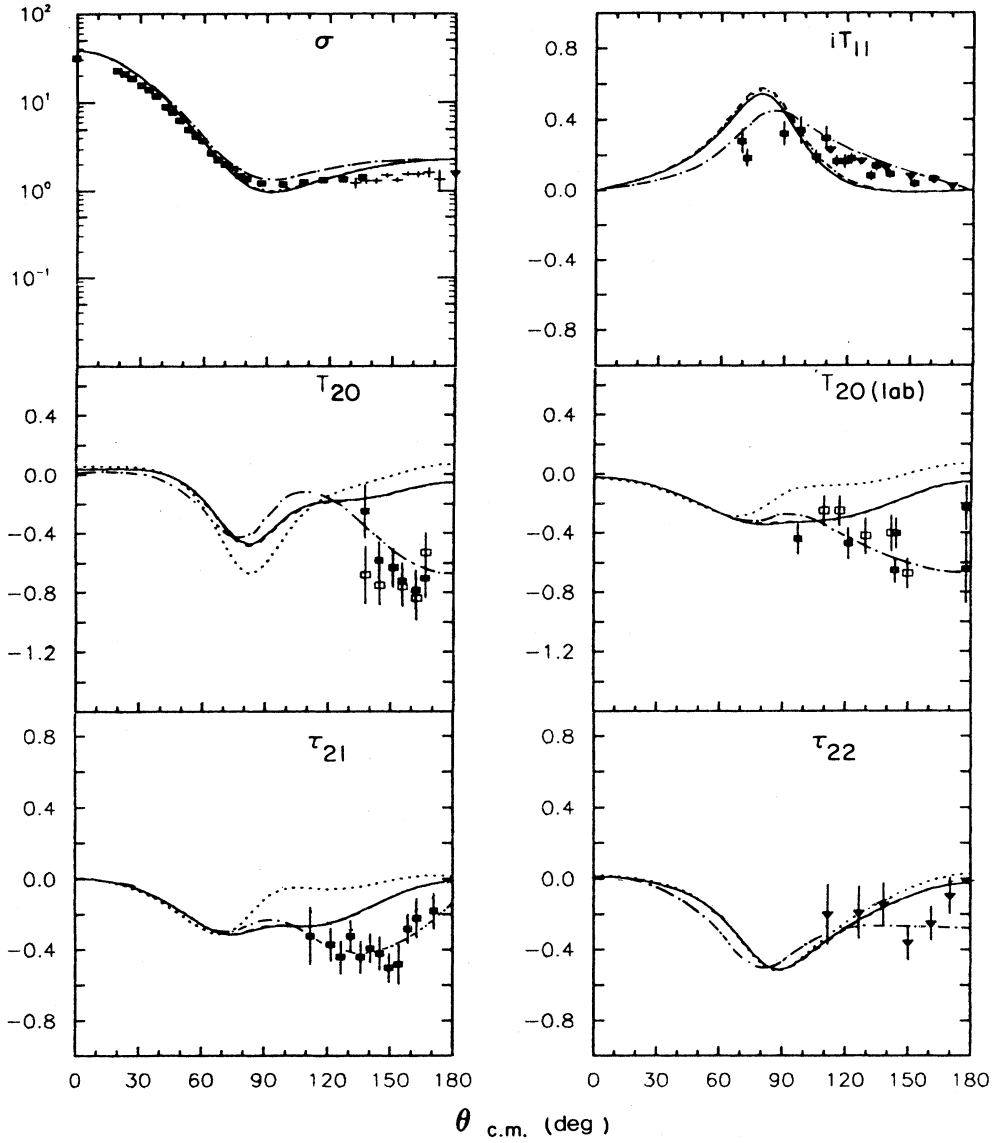

FIG. 8. πd spin observables at $T_\pi^{\text{lab}}=142$ MeV. The curves are standard πNN-NN theory (PNE) of Ref. 10 (dotted line), PNE+(c) correction with S-wave deuteron (dashed line), PNE+(c) correction with $S+D$ deuteron (full line). Here, the full line and dashed line are identical. The dashed-dotted line is the three-body result without the P_{11} contribution. Data are from Refs. 10 and references cited therein. The differential cross section (σ) is in mb/sr.

proved regarding the shape, in particular, around $\theta_{c.m.}=60°$–$100°$. It appears to us that those two quite distinct results are in part related to B helicity amplitude. In fact, when combined with (c) the Flinders model has produced very small $|B|$ at around $\theta_{c.m.}=90°$, which makes it_{11} small in that angular range. The reason behind this is that the Flinders B amplitude has indeed a rather small modulus. In this respect it is worth pointing out that the deuteron D state plays an important role in the correction contribution, as evidenced in it_{11} and to a lesser extent in T_{20} of Figs. 9, 10, and 14.

What we have just discussed above indicates that there

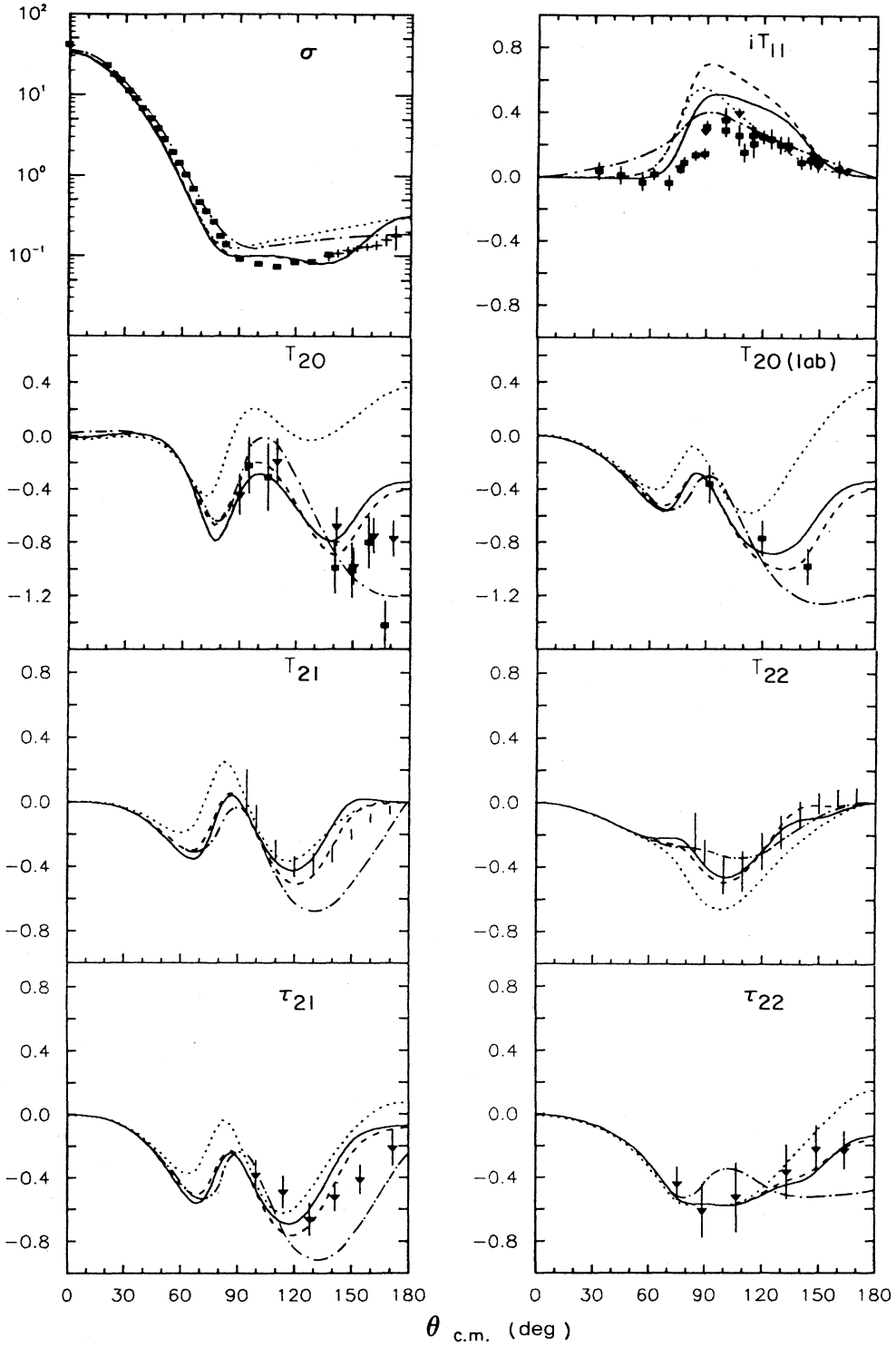

FIG. 9. πd spin observables at $T_\pi^{lab}=256$ MeV. Same legend as in Fig. 8 (full and dashed lines are identical for σ).

still are some degrees of arbitrariness in the choice of the P_{11} input. This, however, may be narrowed down by improving the PNE model prediction in other channels. There is hope for this as data are increasing in, for example, the spin observables in the $NN \rightarrow \pi NN$ (see, for example, Ref. 23).

V. CONCLUSION

Although the model we have adopted for numerical calculation is rather simple, we may safely conclude that we have basically understood the mechanism to improve the description of the πd spin observables, T_{20} in particu-

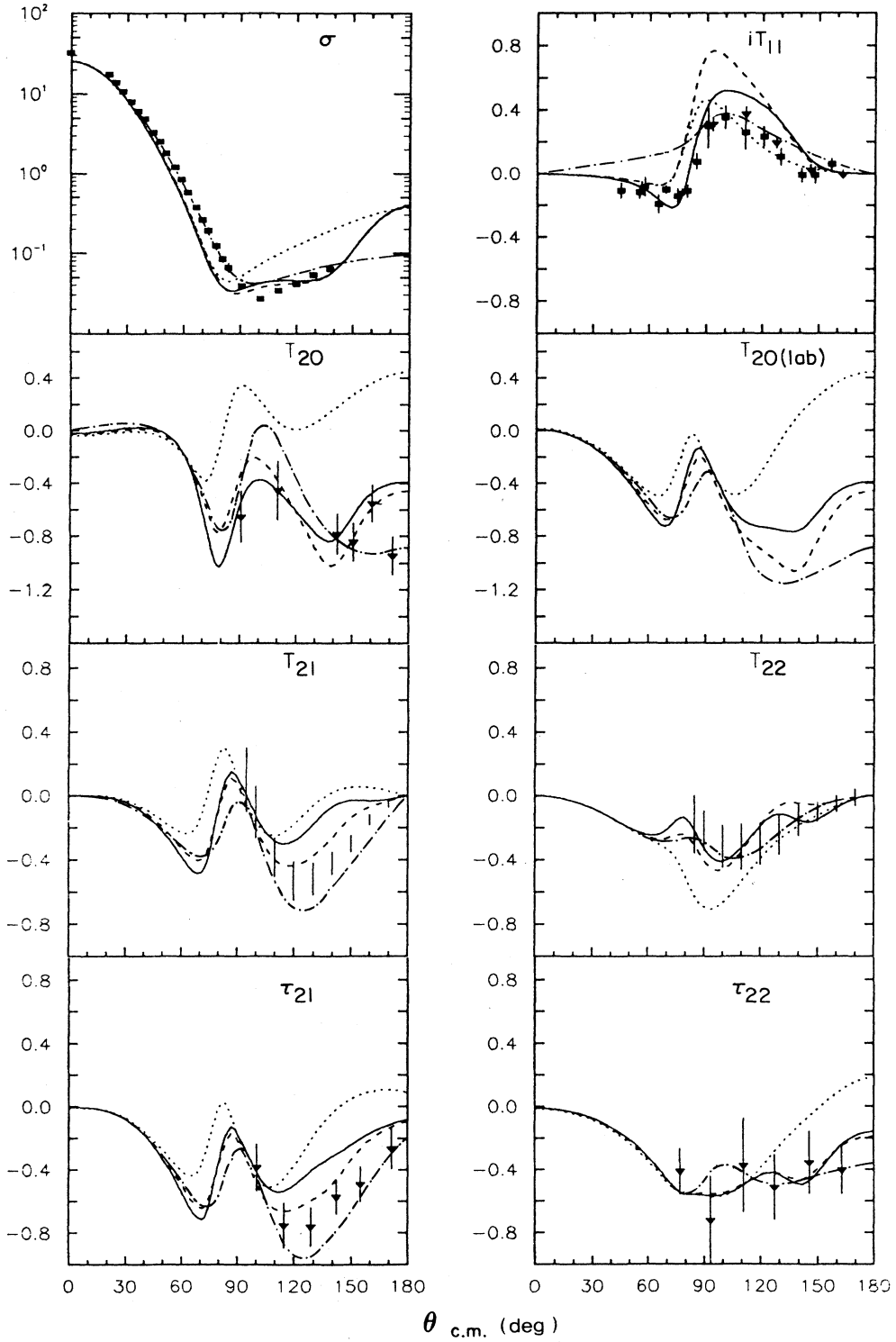

FIG. 10. πd spin observables at $T_\pi^{\text{lab}}=294$ MeV. Same legend as in Fig. 8 (full and dashed lines are identical for σ).

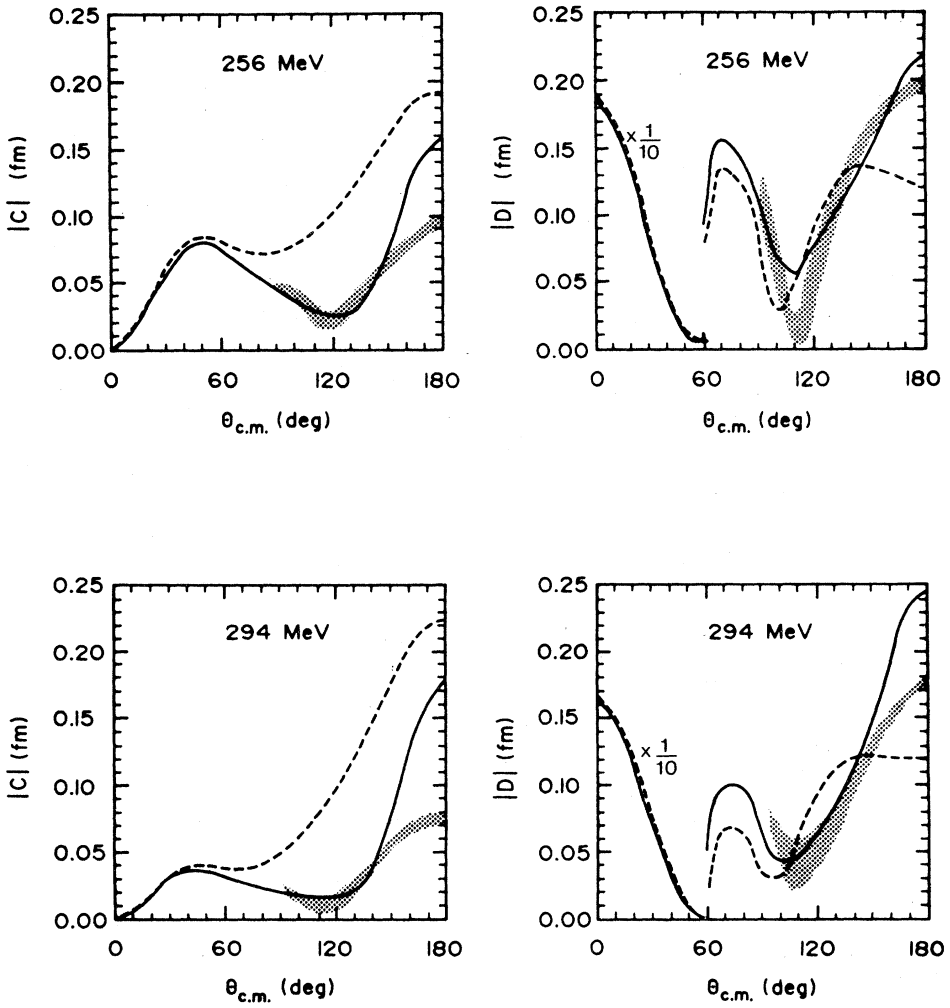

FIG. 11. Moduli of the helicity amplitudes $|C|$ and $|D|$ at 256 and 294 MeV. The curves are PNE+(c) correction with $S+D$ deuteron (full line), and PNE of Ref. 10 (dashed line). Also shown is the amplitude analysis result of Ref. 22 (shadowed band).

lar, in leading order. The mechanism originates from the so-far-neglected contribution from the Pauli exchange process to the covariant πd impulse term through the πN P_{11} state. In a time-ordered theory this contribution is exactly what Jennings proposed to be included in the PNE πd amplitude. So no exotic mechanism like the violation of the Pauli principle needs to be invoked. On the other hand, to make sure that this really is the answer it will be necessary to shape up our theoretical tools for a more complete description of the πd process. In the context of a time-ordered picture, the optimal choice of the P_{11} input is vital, as discussed towards the end of the preceding section. Within this picture many higher order iterates involving the correction mechanism appear to be already included in the original PNE. So we expect the higher order corrections to be small. A typical next order correction that may be somewhat important is indicated by Fig. 12.

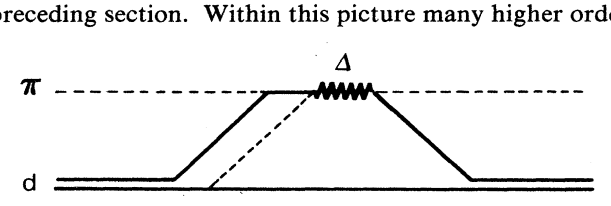

FIG. 12. The next order process corresponding to diagram (c).

Desirably, one would want to perform a more complete calculation within a covariant formulation. As for the lowest order correction one needs to calculate (a^{ex}). For this a reliable model for the πNN and dNN vertex functions for which both nucleons are off mass shell is indispensable. This is a tough requirement, but some attempts seem to be planned so there is some hope for this direction.[24] The corresponding higher order effect is quite hard to assess since the kind of analysis done in Sec. III (and Appendix B) is very difficult to perform when the external particle lines are off shell. We simply hope that our expectation based upon the time-ordered picture may apply to this case as well.

To this end, there are a couple of remarks that need to be addressed. The first point concerns the influence of the correction term (c) in other coupled channels. By observing the diagrammatic expansion of the amplitudes for

those reactions one finds immediately that this correction does not enter either in the lowest or second order terms. Since the process in the energy range of our interest are dominated by the Δ resonance, one sees no reason that its effect is substantial. The second point is that by introducing a parametrized direct (or t-channel) N-Δ interaction in the lowest order into the πd amplitude from the standard three-body calculation Ferreira and Dosch improved the πd observables considerably.[25] It will be interesting to perform this analysis with the PNE amplitudes corrected for diagram (c) to see what the corresponding N-Δ interaction parameters look like.

ACKNOWLEDGMENTS

We are grateful to Prof. E. Boschitz for very useful discussions on the recent πd data from PSI and TRIUMF. We also would like to thank Dr. B. Blankleider for kindly letting us use the Flinders πd amplitudes. One of us (T.M.) is thankful to DPhN/HE, CEN-Saclay, and Institut de Physique Nucléaire de Lyon for their very warm hospitality. This work has been supported in part by the U.S. Department of Energy under Contract No. DE-FG05-84ER40143.

APPENDIX A

The partial wave expansion of the πd helicity amplitudes $H_{\lambda'\lambda}$, where $\lambda(\lambda')=+,0,-$ denotes the initial (final) deuteron helicity $(+1,0,-1)$, is

$$H_{\lambda'\lambda}(\theta,\phi)=e^{-i\phi\lambda}\sum_{Jll'}\sqrt{(2l+1)(2l'+1)}\langle 1\lambda l0|J\lambda\rangle \times\langle 1\lambda' l'0|J\lambda'\rangle f^J_{l'l}d^J_{-\lambda,-\lambda'}(\theta) \quad \text{(A1)}$$

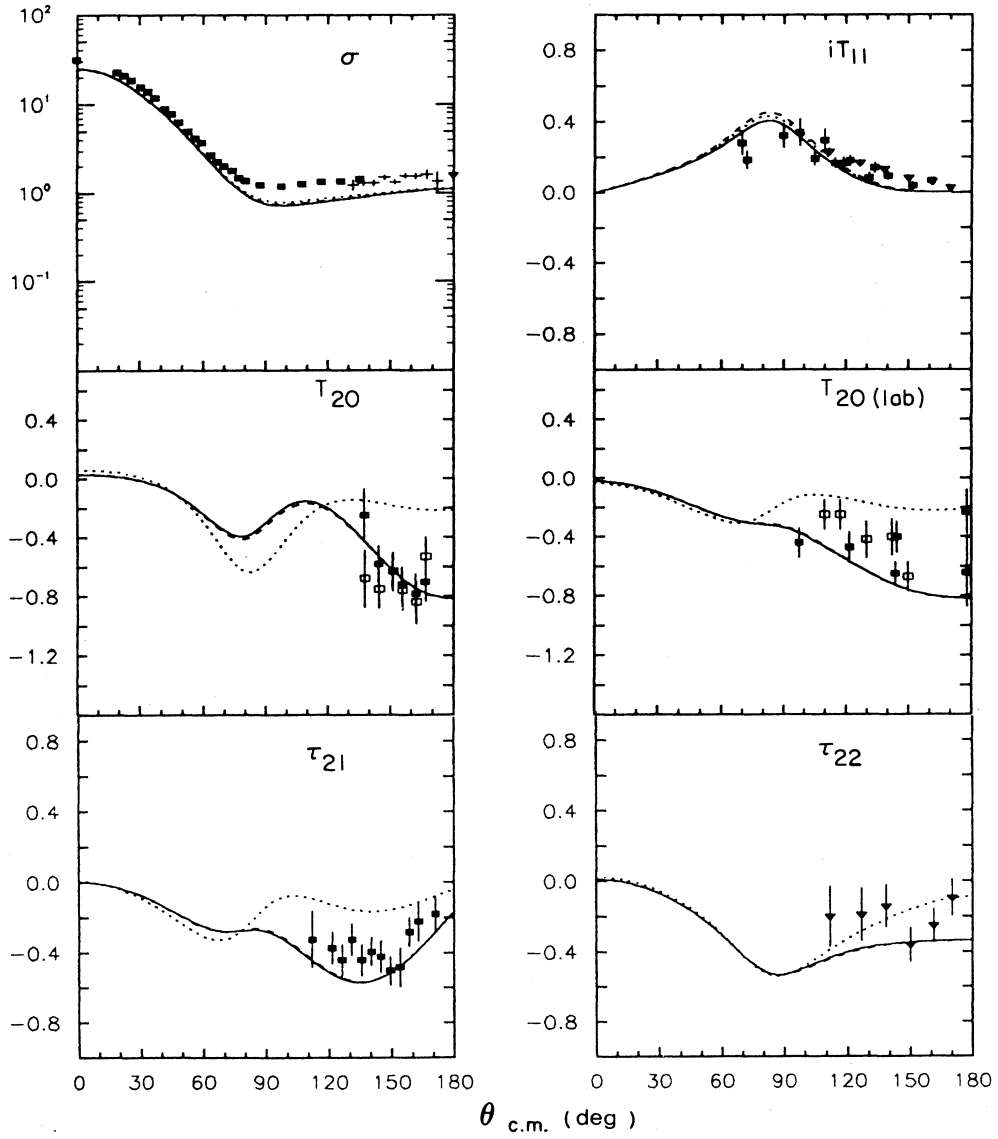

FIG. 13. πd spin observables at $T_\pi^{\text{lab}}=142$ MeV. Same legend as in Fig. 8, but the PNE model is from Flinders, Ref. 2. The results without the P_{11} contribution are not shown here.

where the partial wave amplitudes are defined as

$$f^J_{l'l}=\frac{1}{2ik}[e^{2i\delta^J_{l'l}}-\delta(l',l)] \ . \tag{A2}$$

Here, k is the pion c.m. momentum and $\delta(l',l)$ is the Kronecker symbol.

By parity and time reversal invariance there are four independent amplitudes:

$$\begin{aligned} A &= H_{++}=H_{--} \ , \\ B &= H_{+0}=H_{0-}=-H_{0+}=-H_{-0} \ , \\ C &= H_{+-}=H_{-+} \ , \\ C &= H_{00} \ . \end{aligned} \tag{A3}$$

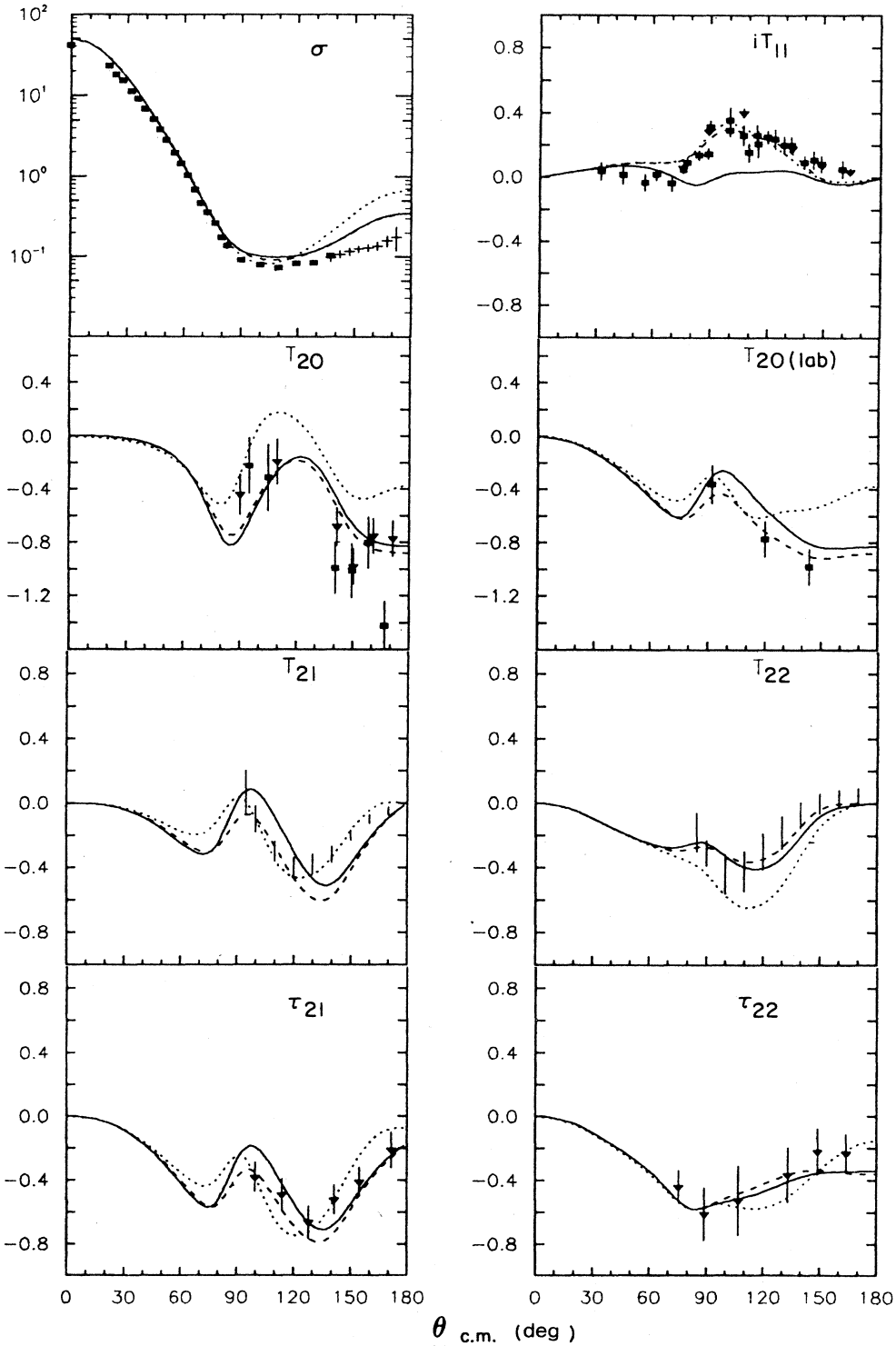

FIG. 14. πd spin observables at $T_\pi^{\rm lab}=256$ MeV. Same legend as in Fig. 13.

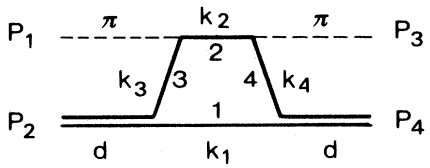

FIG. 15. The kinematical situation corresponding to diagram (*a*) of Fig. 3.

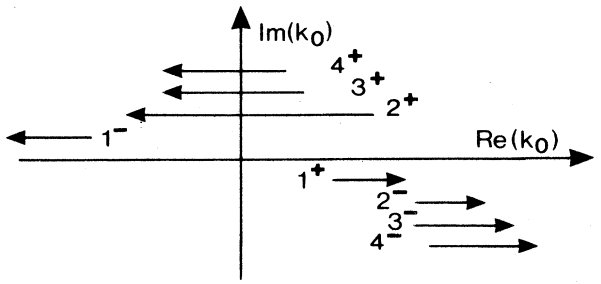

FIG. 16. The position in the complex-k plane of the poles of the nucleon propagators of Fig. 15.

The explicit forms of these amplitudes in terms of the partial wave amplitudes are

$$A=\tfrac{1}{2}\sum_{J\geq 1}\{(J+1)f^J_{J-1,J-1}+Jf^J_{J+1,J+1}+(2J+1)f^J_{J,J}+2[J(J+1)]^{1/2}f^J_{J-1,J+1}\}d^J_{1,1}(\theta)\ ,$$

$$B=-\tfrac{1}{2}\sum_{J\geq 1}\{[2J(J+1)]^{1/2}(f^J_{J+1,J+1}-f^J_{J-1,J-1})+\sqrt{2}f^J_{J-1,J+1}\}d^J_{1,0}(\theta)\ ,$$

$$C=\tfrac{1}{2}\sum_{J\geq 1}\{(J+1)f^J_{J-1,J-1}-+Jf^J_{J+1,J+1}-(2J+1)f^J_{J,J}+2[J(J+1)]^{1/2}f^J_{J-1,J+1}\}d^J_{1,-1}(\theta)\ ,$$

$$D=\sum_{J\geq 0}\{Jf^J_{J-1,J-1}+(J+1)f^J_{J+1,J+1}-2[J(J+1)]^{1/2}f^J_{J-1,J+1}\}d^J_{0,0}(\theta)\ . \tag{A4}$$

The c.m. differential cross section is

$$\frac{d\sigma}{d\Omega}=\tfrac{1}{3}\Sigma,\quad \Sigma=2|A|^2+4|B|^2+2|C|^2+|D|^2\ . \tag{A5}$$

The final state vector and tensor observables are in the Madison convention:

$$\begin{aligned} it_{11}&=\sqrt{6}\,\mathrm{Im}[B^*(A-C+D)]/\Sigma\ ,\\ T_{20}&=\sqrt{2}(|A|^2+|C|^2-|B|^2-|D|^2)/\Sigma\ ,\\ T_{21}&=\sqrt{6}\,\mathrm{Re}[B^*(A-C+D)]/\Sigma\ ,\\ T_{22}&=\sqrt{3}[2\,\mathrm{Re}(A^*C)-|B|^2]/\Sigma\ . \end{aligned} \tag{A6}$$

APPENDIX B

Here we shall explain in somewhat more detail how diagram (*c*) (or the Jennings term) comes about in the covariant PNE. As stated in Sec. III we simplify the problem by using S-wave πNN and NNd vertices which are of zero range (point vertex) together with the assumption that all the particles involved are scalars. Also the nucleon propagators are taken as undressed. These simplifications do not alter the conclusion that we want to draw.

First we consider the process corresponding to diagram (*a*). We choose the πd c.m. frame and the corresponding kinematical situation is depicted in Fig. 15 where the four on-shell four-momenta are

$$\begin{aligned} P_1&=(\omega,\mathbf{p}),\quad P_2=(D,-\mathbf{p})\ ,\\ P_3&=(\omega,\mathbf{q}),\quad P_4=(D,-\mathbf{q})\ , \end{aligned} \tag{B1}$$

with

$$\begin{aligned} \omega&=(p^2+\mu^2)^{1/2}=(q^2+\mu^2)^{1/2}\ ,\\ D&=(p^2+M_d^2)^{1/2}=(q^2+M_d^2)^{1/2}\ , \end{aligned} \tag{B2}$$

where $p=|\mathbf{p}|=|\mathbf{q}|=q$, and μ and M_d are the pion and deuteron rest masses. The total c.m. energy is therefore $W=\omega+D$.

The loop momenta are

$$\begin{aligned} k_1&=(k_0,\mathbf{k}),\quad k_2=(W-k_0,-\mathbf{k})\ ,\\ k_3&=k_2-P_1=(D-k_0,-\mathbf{k}-\mathbf{p})\ ,\\ k_4&=k_2-P_3=(D-k_0,-\mathbf{k}-\mathbf{q})\ . \end{aligned} \tag{B3}$$

The amplitude corresponding to the figure is proportional to the following integral:

$$I=\int dk_0 d\mathbf{k}\, gv\frac{1}{(k_3^2-m^2+i\epsilon)(k_1^2-m^2+i\epsilon)(k_2^2-m^2+i\epsilon)(k_4^2-m^2+i\epsilon)}vg\ , \tag{B4}$$

where m is the nucleon mass, and g and v are the πNN and NNd vertices, respectively. Each nucleon propagator admits one positive- and one negative-energy pole. They are identified as $j^{\pm}$ ($j=1$–4) and their locations are

$$\begin{aligned} &1^{\pm}:\ k_0=\pm(E_k-i\epsilon),\quad 2^{\pm}:\ k_0=W\mp(E_k-i\epsilon)\ ,\\ &3^{\pm}:\ k_0=D\mp(E_{k+p}-i\epsilon)\ ,\\ &4^{\pm}:\ k_0=D\mp(E_{k+q}-i\epsilon)\ , \end{aligned} \tag{B5}$$

where $E_{k+p}=[m^2+(\mathbf{k}+\mathbf{p})^2]^{1/2}$. Here $i\epsilon$ specifies whether a specific pole in consideration is in the upper or lower half complex-k plane. The situation is shown in Fig. 16.

In Fig. 16, the arrows indicate the motion of the poles with increasing $|\mathbf{k}|$. Strictly speaking the poles in propagators 3 and 4 are nonmonotonic functions until $|\mathbf{k}|$ becomes sufficiently large as compared with $|\mathbf{p}|$ or $|\mathbf{q}|$.

The integral in k_0 may be augmented by a half circle

with an infinite radius either in the upper or lower half plane which gives the identical result with the original integral. By anticipating the result which, in the limit, reduces to the nonrelativistic situation, we choose to close the contour in the lower half plane. Then the integral gets contributions from four poles: 1^+, 2^-, 3^-, and 4^- of which only 1^+ is the positive-energy pole. The contributions from the remaining negative-energy poles are small and can therefore be neglected. The so-called spectator on-shell approximation is just to retain the residue of this positive-energy pole. Clearly nucleon 1 is the spectator put on mass shell in the presence of the πN interacting through the P_{11} pole term. Then the integral I above becomes

$$I \simeq -i\pi \int \frac{d\mathbf{k}}{E_k} \psi^*(P_2,\tilde{k}) g \frac{1}{(W-E_k)^2-E_k^2} g \psi(P_4,\tilde{k}) , \tag{B6}$$

with $\tilde{k}=(E_k,\mathbf{k})$ and where

$$\psi(P_2,\tilde{k})=\frac{v}{(P_2-\tilde{k})^2-m^2} \tag{B7}$$

may be identified as the deuteron wave function. The energy denominator is

$$(W-E_k)^2-E_k^2=(W-2E_k)W , \tag{B8}$$

so finally

$$I \simeq \int d\mathbf{k} \frac{\psi^* g g \psi}{W-2E_k} , \tag{B9}$$

which is essentially the contribution from diagram (a) in the main text in the time-ordered approach.

A few remarks may be due concerning some small details of the above calculation.

(i) Before the $\mathbf{k}$ integration is done the ratio of negative-energy 2^- pole contribution to that from the positive-energy 1^+ pole is roughly $(W-2E_k)/(W+2E_k)$. In a calculation with realistic deuteron and πNN vertices the contribution from large values of $|\mathbf{k}|$ is suppressed particularly by the deuteron vertex and the $\mathbf{k}$ integration is dominated by the contribution from the value around $|\mathbf{k}| \sim |\mathbf{p}|$ or $|\mathbf{q}|$. Then the ratio becomes $\sim(D+\omega-2E_p)/(D+\omega+2E_p)$. For the values of $|\mathbf{p}|$ of our interest, πd scattering in the Δ resonance region, this ratio is not far from $\omega/(2D+\omega)$, and is quite small.

(ii) It can be shown that $E_k > D-E_{k+p}$, and $E_k > D-E_{k+q}$, so no pinching singularity occurs due to 1^+ and 3^+, or 1^+ and 4^+.

(iii) On the contrary 1^+ and 2^+ pinch the k_0 integration contour, which eventually gives the energy denominator $(W-2E_k)$, corresponding to the two-nucleon elastic unitarity cut.

(iv) For the forward scattering, $\mathbf{p}=\mathbf{q}$, 3^- and 4^- poles coincide and their residue contributions cancel exactly. Even for the nonforward scattering those contributions tend to compensate each other making the negative-energy pole contributions even smaller.

(v) For certain values of $\mathbf{k}$, 2^- and 3^- (or 4^-) poles coincide. Here again their residues cancel each other. In this way the dominance of the positive-energy pole contribution is always maintained.

Now we shall study the covariant process corresponding to diagram (a^{ex}). This is depicted in Fig. 17 below. The notations are almost the same as those defined above except for those loop momenta k_5, k_6, k_7, and k_8 defined as

$$\begin{aligned} &k_5=(k_0,\mathbf{k}), \quad k_6=(W-k_0,-\mathbf{k}) , \\ &k_7=P_2-k_5=(D-k_0,-\mathbf{p}-\mathbf{k}) , \\ &k_8=P_3-k_5=(\omega-k_0,\mathbf{q}-\mathbf{k}) . \end{aligned} \tag{B10}$$

The amplitude corresponding to this diagram involves an integration over k_0 and $\mathbf{k}$ just like the expression for I above. The integrand is basically a product of four nucleon propagators:

$$\frac{1}{k_j^2-m^2+i\epsilon} \quad (j=5\rightarrow 8) . \tag{B11}$$

Just as before the poles corresponding to the four-nucleon propagators are identified as

$$\begin{aligned} &5^{\pm}: \ k_0=\pm(E_k-i\epsilon), \quad 6^{\pm}: \ k_0=W\mp(E_k-i\epsilon) , \\ &7^{\pm}: \ k_0=D\mp(E_{k+p}-i\epsilon) , \\ &8^{\pm}: \ k_0=\omega\pm(E_{k-q}-i\epsilon) . \end{aligned} \tag{B12}$$

The above notations are the same as the previous ones except that

$$E_{k-q}=[m^2+(\mathbf{k}-\mathbf{q})^2]^{1/2} .$$

The pole positions are illustrated in Fig. 18.

With some simple algebra it is easy to show that (i) poles 6^- and 7^- may coincide in which case their residues cancel exactly, and (ii) 5^+ and 6^+ may pinch the integration contour, but that no other coincidence of poles can be expected. Upon closing the k_0 integration in the lower half plane one picks up two positive-energy pole contributions. The first one is due to 5^+ which, one can show easily, corresponds to (a^{ex}) calculated within the time-ordered picture, and is the Pauli exchange term to the contribution I evaluated above within the spectator on-shell approximation. Needless to say, this obtains the energy denominator $W-2E_k$. Now the contribution from the second positive-energy pole 8^+ has no counterpart in the previous diagram (a). Upon taking the residue at this pole we find that the contribution to the am-

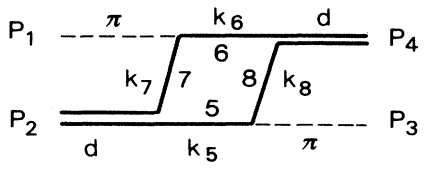

FIG. 17. The kinematical situation for the covariant process corresponding to diagram (a^{ex}) of Fig. 3.

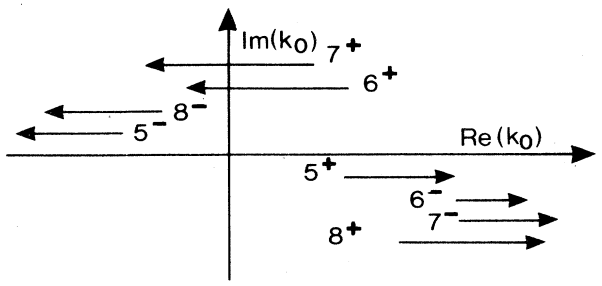

FIG. 18. The position in the complex-k plane of the poles of the nucleon propagators of Fig. 17.

plitude is proportional to

$$J=-i\pi\int\frac{d\mathbf{k}}{E_{k-q}}\psi^*(P_2,\tilde{k})g \times\frac{1}{(D-\omega-E_{k-q})^2-E_{k+p}^2}g\psi(P_4,\tilde{k}) , \quad \text{(B13)}$$

where $\tilde{k}=(D-E_{k-q},-\mathbf{k})$.

The energy denominator in the above expression which comes from propagator 7 may be decomposed into two parts:

$$\frac{1}{2E_{k+p}}\left[\frac{1}{D-\omega-E_{k-q}-E_{k+p}} -\frac{1}{D-\omega-E_{k-q}+E_{k+p}}\right] . \quad \text{(B14)}$$

The first term in the bracket is the 8^+ residue containing the positive-energy part of the propagator 7 while the second term combines with the negative-energy part of the propagator. The latter gives a smaller contribution relative to the first one. When we drop this latter term and use the on-shell condition $W=D+\omega$ the first term becomes

$$\frac{1}{2E_{k+p}}\frac{1}{(W-\omega_p-\omega_q-E_{k-q}-E_{k+p})} , \quad \text{(B15)}$$

where $\omega_p=\omega_q=\omega$.

Then the contribution to the t matrix from the pole 8^+ becomes

$$J\simeq\int d\mathbf{k}\psi^*g\frac{1}{W-\omega_p-\omega_q-E_{k-q}-E_{k+p}}g\psi . \quad \text{(B16)}$$

Now it is easy to find that this corresponds to the diagram (c) in the time-ordered picture.

We have thus demonstrated that the covariant PNE naturally contains the diagram (c), suggested by Jennings.

[1]Y. Avishai and T. Mizutani, Nucl. Phys. **A326**, 352 (1979); **A338**, 337 (1980); **A352**, 399 (1981); Phys. Rev. C **27**, 312 (1983).
[2]I. R. Afnan and B. Blankleider, Phys. Rev. C **22**, 1638 (1980); B. Blankleider and I. R. Afnan, *ibid.* **24**, 1572 (1981); **31**, 1380 (1985).
[3]A. W. Thomas and A. S. Rinat, Phys. Rev. C **20**, 216 (1979); A. S. Rinat and Y. Starkand, Nucl. Phys. **A397**, 381 (1983).
[4]H. Garcilazo and T. Mizutani, Few-Body Systems **5**, 127 (1988).
[5]T. Mizutani, B. Saghai, C. Fayard, and G. H. Lamot, Phys. Rev. C **35**, 667 (1987).
[6]J. Holt *et al.*, Phys. Rev. Lett. **43**, 1229 (1979); **47**, 472 (1981); E. Ungricht *et al.*, *ibid.* **52**, 333 (1984); Phys. Rev. C **31**, 934 (1985).
[7]Y. M. Shin *et al.*, Phys. Rev. Lett. **55**, 2672 (1985); N. R. Stevenson *et al.*, Phys. Rev. C **39**, 1488 (1989).
[8]H. Garcilazo, Phys. Rev. C **35**, 1804 (1987).
[9]I. R. Afnan and R. J. McLeod, Phys. Rev. C **31**, 1821 (1985).
[10]G. H. Lamot, J. L. Perrot, C. Fayard, and T. Mizutani, Phys. Rev. C **35**, 239 (1987).
[11]G. R. Smith *et al.*, Phys. Rev. Lett. **57**, 803 (1986); Phys. Rev. C **38**, 251 (1988); **38**, 2427 (1988).
[12]C. R. Ottermann *et al.*, Phys. Rev. C **38**, 2296 (1988); **38**, 2310 (1988).
[13]B. K. Jennings, Phys. Lett. B **205**, 187 (1988).
[14]B. K. Jennings and A. S. Rinat, Nucl. Phys. **A485**, 421 (1988).
[15]W. Grein and M. P. Locher, J. Phys. G **7**, 1355 (1981).
[16]T. Mizutani, C. Fayard, G. H. Lamot, and R. S. Nahabetian, Phys. Rev. C **24**, 2633 (1981).
[17]A. T. Stelbovics and M. Stingl, Nucl. Phys. **A249**, 391 (1978); J. Phys. G **4**, 1371 (1978); **4**, 1389 (1978).
[18]I. R. Afnan and A. T. Stelbovics, Phys. Rev. C **23**, 1384 (1981).
[19]N. Nakanishi, Prog. Theor. Phys. Suppl. **43**, 1 (1969).
[20]F. Gross, Phys. Rev. C **26**, 2203 (1982).
[21]J. Haidenbauer and W. Plessas, Phys. Rev. C **30**, 1822 (1984).
[22]H. Garcilazo *et al.*, Phys. Rev. C **39**, 942 (1989).
[23]R. L. Shypit *et al.*, Phys. Rev. Lett. **60**, 901 (1988).
[24]F. Gross, private communication.
[25]E. Ferreira and H. G. Dosch, Univ. Pontifica (Brazil) report, 1988.